Journal of Power Sources 184 (2008) 251–259

Contents lists available at ScienceDirect

Journal of Power Sources

journal homepage: www.elsevier.com/locate/jpowsour

Degradation measurement and analysis for cells and stacks

Randall S. Gemmen [a,*], Mark C. Williams [b,1], Kirk Gerdes [c,2]

[a] Fuel Cell Research, National Energy Technology Laboratory, 3610 Collins Ferry Road, Morgantown, WV 26507, United States
[b] URS/EG&G, National Energy Technology Laboratory, 3610 Collins Ferry Road, Morgantown, WV 26507, United States
[c] National Energy Technology Laboratory, 3610 Collins Ferry Road, Morgantown, WV 26507, United States

ARTICLE INFO

Article history:
Received 18 April 2008
Received in revised form 10 June 2008
Accepted 11 June 2008
Available online 25 June 2008

Keywords:
Degradation
Fuel cell
Standards
ASR
Area-specific resistance

ABSTRACT

Past research in solid oxide fuel cell (SOFC) performance assessment and improvement has focused on cell operating voltage (efficiency). Related to this metric, but distinct and equally important, is performance degradation. This paper examines cell degradation, provides key definitions needed for its characterization, and discusses the relationship of various cell performance variables. To characterize degradation, two parameters are defined, namely, area-specific resistance (ASR), and degradation rate (DR). The ASR of a cell/stack increases as a result of degradation, and therefore needs to be modeled as a time-dependent parameter. A model for SOFC cell performance is used to describe polarization losses, and to predict degradation performance. The model is then used to demonstrate the use of ASR and DR in the assessment of degradation. Available experimental data is separately used to do the same. ASR is shown to be insensitive to certain variations in test conditions and therefore is the preferred parameter for fuel cell developers when comparing performance differences arising from incremental changes in design/materials. DR is the preferred parameter for determining changes in efficiency over the lifetime of the cell/stack, which is a key concern for end users.

Published by Elsevier B.V.

1. Introduction

The promotion and marketing of power generation, regardless of technology, requires demonstrated ability to convert fuel to electric energy at low amortized cost. Given the high capital costs of most fuel cell technologies, low amortized costs can only be achieved with long lifetimes. Hence, degradation behavior remains a key development concern for all fuel cell types (PEMFC, AFC, PAFC, SOFC, MCFC, etc.). An example of such degradation, determined experimentally, is shown in Fig. 1 for a solid oxide fuel cell (SOFC) system operated on a fuel mixture of hydrogen and carbon monoxide. The time averaged degradation rate in *system efficiency* was approximately 3% per 1000 h.

An example of degradation at the *cell level* is shown in Fig. 2. Here, the degradation behavior of an SOFC button cell operated on simulated coal syngas containing a trace element from coal (0.5 ppm H_2Se) was assessed. Such studies are necessary to characterize the limits of trace element exposure for coal-based SOFC power generation. Viable SOFC operation on coal will be possible with proper clean-up of syngas once such specifications are defined. Introduction of trace coal elements (e.g., selenium, arsenic, cadmium, phosphorous, etc.) into the fuel matrix provides an additional set of material interaction mechanisms by which degradation may proceed. Such mechanisms may proceed more rapidly compared to those when operating on pure hydrogen, thereby reducing the lifetime of the cell. It is also possible that a given degradation mechanism will be partially or completely reversible, and thereby allow for cell recovery and additional lifetime. As shown in Fig. 2, for SOFC operation on coal syngas with 0.5 ppm H_2Se, there was an instantaneous drop in cell voltage upon H_2Se injection, followed by a slower rate of decay until the voltage reached 0.68 V. Also shown in Fig. 2 is the average degradation rate determined from the voltage data using a methodology to be discussed in Section 3.

These examples represent the present status of fuel cell degradation characterization. Improved analysis methods and characterization parameters are needed that will allow improved understanding of the observed behavior.

1.1. Present understanding of degradation mechanisms

As summarized below, past examination and analysis of degradation has occurred at system and subcomponent scales using

* Corresponding author. Tel.: +1 304 285 4536; fax: +1 304 285 0903.
E-mail addresses: randall.gemmen@netl.doe.gov (R.S. Gemmen), mark.willams@eg.netl.doe.gov (M.C. Williams), kirk.gerdes@netl.doe.gov (K. Gerdes).
[1] Tel.: +1 304 285 4344; fax: +1 304 285 0903.
[2] Tel.: +1 304 285 4342; fax: +1 304 285 0903.

0378-7753/$ – see front matter. Published by Elsevier B.V.
doi:10.1016/j.jpowsour.2008.06.047

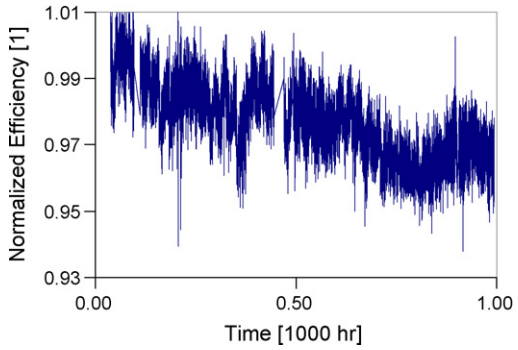

Fig. 1. Degradation of a nominal 5 kW solid oxide fuel cell system, Gemmen [1].

various experimental and modeling methods. Degradation in all fuel cell technologies (solid oxide, polymer electrolyte, molten-carbonate, alkaline, etc.) has been assessed in a limited way, with each fuel cell type having unique mechanistic behaviors, as well as features common to other fuel cell types. Common features include electrode contact loss and increased contact resistance, changes in material composition and structure including grain coarsening, interdiffusion, phase changes, and deactivation of catalysts (after Steinberger-Wilckens et al. [2]).

Mazumder et al. [3] provides a method of systems-level modeling for the effects of power conditioning and load on SOFC performance. The work identified that certain power conditioner types may be detrimental to SOFC operation. Further modeling work has been done at the cell level to examine effects of sintering of nickel during SOFC operation, Ioselevich et al. [4]. For polymer electrolyte membrane fuel cell (PEFC) technology, Kulikovsky et al. [5] propose that cell degradation occurs as a wave over the cell which effectively removes active area over time. They provide a phenomenological model for these effects, and then predict cell degradation performance. Fowler et al. [6] provide a generalized model that treats three proposed degradation methods in PEFC technology; namely, electrolyte humidification, catalytic activation loss, and mass transfer losses.

Experimental work on the degradation of ceramic and polymer electrolyte systems has also been performed by Haeringa et al. [7] and Meyer et al. [8], respectively. Haeringa et al. [7] suggest that a transformation of defects occurs in 8% YSZ which causes the decrease in conductivity over time. Meyer et al. [8] identified a thermo-activated chemical degradation mechanism for sulfonated polyimide membranes. De Castro [28] summarizes several physical degradation mechanisms of polymer membranes: mechanical degradation via excessive water swelling, high localized stress, MEA processing resulting in cracking, tearing, perforations, and blistering; thermo-hydrolytical degradation via de-sulfonation and chain scission; and chemical attack by free radicals via HO· and HOO on the anode, and H_2O_2 on the cathode.

Numerous experimental investigations of electrode degradation for a variety of technologies have also been performed. Schulze and Christenn [9] showed how the hydrophobicity of PEFC electrodes evolves with time as the hydrophobic agent, polytetrafluoro-ethylene, degrades. As the hydrophobicity changes in time, an initial increase in performance is seen, but then the performance decreases as operation continues. Chen et al. [10] showed how direct methanol fuel cells degrade as the particle size of the electrocatalysts increases with time. Schulze and Gülzow [11] showed the degradation of alkaline fuel cells due to disintegration of nickel anodes. Taniguchi et al. [12] showed how SOFC electrode–electrolyte interfaces can be deactivated due to chromium evolved from metal interconnects. Hagen et al. [27] determined the effect of operating temperature and cell polarization on anode supported SOFC degradation rate. They find that higher rates of degradation occur for lower temperatures and higher overpotentials. Other work has also suggested that conductive pastes in SOFC technology, Chervin et al. [13], and specific operational conditions in PEMFC technology, Taniguchi et al. [14], may also cause degraded fuel cell performance.

The fuel source, composition, quality, and presence of trace impurities affect cell lifetime. For example, sulfur compounds are contained in most commercial fuels. Matsuzaki and Yasuda [15] show that SOFC nickel anodes can be poisoned to different extents depending on exposure time, temperature and sulfur concentration. However, Aguilar et al. [16] show that degradation of SOFC's operated on sulfur containing fuels can be potentially mitigated with advances in new anode material.

Structural degradation can also impact cell performance. Weil et al. [17] show how seal materials degrade (causing delamination along the electrolyte) on SOFC systems which can then cause a loss in voltage potential as reactant gases directly oxidize rather than react electrochemically.

Over-utilization of fuel can lead to oxidation of the anode material at the electrolyte–anode interface. Fig. 3 shows an example of this process for a cell having a Ni/YSZ anode and YSZ electrolyte. Note that at 80% fuel utilization (97% H_2, 3% H_2O) the performance of the cell reaches a steady-state with very small or no degradation resolvable over the noise in the signal, while at 85% utilization the cell degrades more rapidly (ca. 52% per 1000 h). Continued

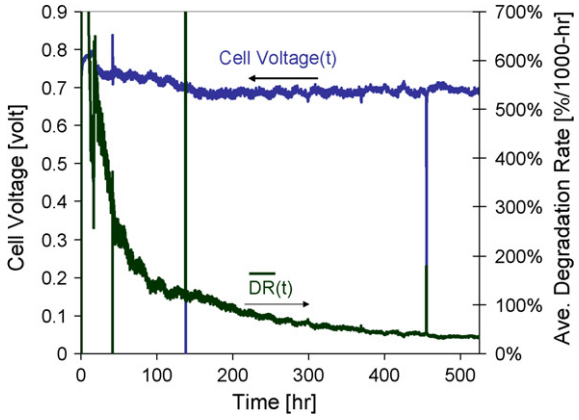

Fig. 2. Voltage degradation of Ni/YSZ anode supported SOFC button cell upon exposure (at $t = 17$ h) to 0.5 ppm H_2Se in coal syngas. Current density = 0.25 A cm^{-2}; fuel = 29% H_2, 29% CO, 12% CO_2, 3% N_2, and 27% H_2O; temperature = 800 °C. Also shown is the average degradation rate calculated via Eq. (8).

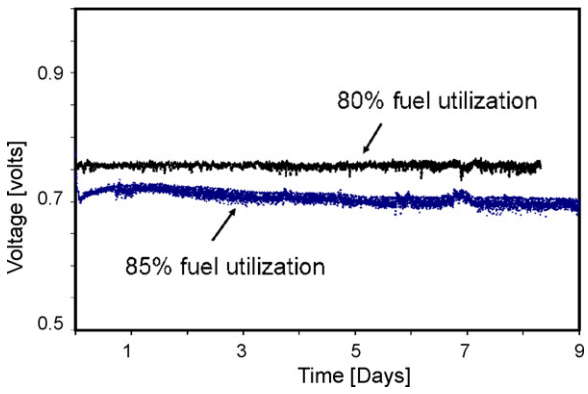

Fig. 3. Voltage vs. time for cells run at a fuel utilizations of 80 and 85%, Gemmen and Johnson [18].

severe degradation by this mode can lead to delamination of the anode–electrolyte interface.

Regarding stack operation more particularly, it is widely recognized that all fuel cell types require proper management of flow and temperature to avoid degradation. Ideally, uniform flow and temperature conditions can achieve peak stack performance. Significant departure from such uniform conditions can result in material phase changes (oxidation of anode materials, or reduction of cathode materials), or thermal degradation (sintering) as discussed previously.

1.2. Technical objective

The objective of this work is to document a consistent method for assessing degradation at the cell/stack level. The need for such a method is noted by Steinberger-Wilckens et al. [2] and Steinberger-Wilckens et al. [19]. The development of a degradation performance parameter for the cell/stack level is similar to that being pursued at the system level, Gemmen and Johnson [18]. In the present work, we employ a SOFC model to quantitatively estimate several polarization losses and predict cell degradation. These model data, showing degradation behavior representative of actual systems, are used to demonstrate the proposed degradation assessment. Separately, available experimental data are used to demonstrate the same on real-world data.

1.3. Paper overview

In Section 2, a summary of present concerns is given for how degradation performance is measured. In Section 3, an analysis for fuel cell degradation is presented, and a method is proposed for assessing the degradation of a cell/stack. Section 4 employs an empirical model to demonstrate the method being proposed. Section 5 further demonstrates the proposed method using available experimental data. Finally, Section 6 provides a closing discussion on degradation and the proposed assessment method, and Section 7 provides the summary and conclusions of the key results.

2. Present issues/concerns in the measurement of degradation

As evident from Section 1, fundamental molecular and microstructural evolutions have been identified and proposed to explain degradation, and undoubtedly future work will identify more. However, in situ methods to directly probe degradation modes and quantify their evolution over time do not yet exist, and only indirect cell/stack performance 'indicators' are available. These indicators are the measured voltages across the cell by various techniques such as fixed current, ac-current impedance techniques, and step-change current techniques.

2.1. Issues in the measurement of degradation

Presently, only *overall* performance metrics (overall cell voltage or system efficiency) are available to researchers as a way to measure performance changes, and infer the existence of at least one of the aforementioned degradation mechanisms. For example, Gemmen and Johnson [18] discuss the degradation assessment at the fuel cell *system level*, showing how system efficiency degradation can be used to characterize performance *provided* careful system tests are performed. As explained by Gemmen and Johnson [18], understanding *how* the test is performed is critical since the system designer/operator can trade off efficiency performance for degradation performance during operation. In this paper, we treat degradation at the cell/stack level, and propose to employ certain

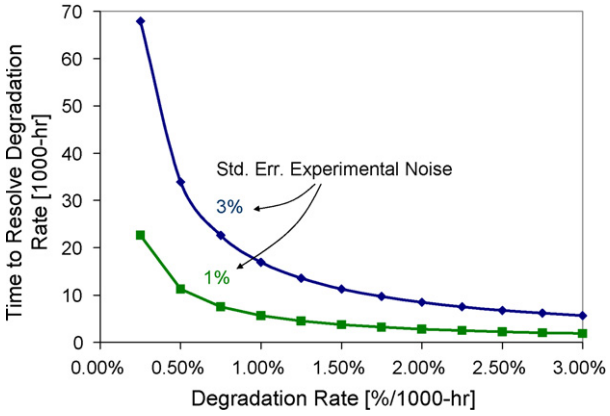

Fig. 4. Test duration required to experimentally resolve true degradation rate vs. nominal degradation rate-degradation calculated from voltage difference between starting and ending points. Assumes a standard error of the experimental noise = 3 and 1%, and a standard error in the measured degradation rate = 25%. Results show that efforts to reduce experimental noise permit proportional reduction in required test duration.

cell/stack voltage measurements and analysis methods to assess cell/stack degradation.

Rapid technology advances have reduced degradation rates to less than 1% per 1000 h. The implication for developers with mature technology is that measuring performance improvements due to incremental changes in design or materials can be difficult and expensive owing to the increased data sensitivity requirements and/or extended test durations. Statistically significant resolution of the differences between two cell designs now requires thousands of hours of precise testing. Fig. 4 shows the time required to resolve (to within 25%) the true degradation of a cell as a function of the degradation rate. Since experimental noise is largely fixed, as technology improves and degradation is decreased, longer test durations are required to accurately measure the true degradation. In short, the signal to noise ratio for this problem is getting smaller with each reduction of the degradation rate. Aside from electrical instrumentation noise, other primary sources of noise/variation are experimental temperature, pressure and reactant concentration. A degradation performance parameter (or parameters) that mitigates the influence of such experimental 'noise' on the degradation measurement is needed.

In Section 3, a definition of area-specific resistance (ASR) is proposed to achieve the objective of reduced noise sensitivity. We show that there are two parameters that are useful in degradation research, one being the cell (or component) ASR, and the other is the rate at which such resistance increases thereby causing performance degradation—called the degradation rate (DR) of the cell.

2.2. Separation of voltage losses

As explained, voltage measurements are used to evaluate cell degradation. Five distinct losses commonly characterize the voltage performance of a cell: (a) *ohmic voltage loss*—the voltage drop associated with the resistance of the electrolyte, the electrodes, the interconnect, and the contact regions between the electrodes and the interconnect; (b and c) *cathode and anode concentration polarization*—the theoretical voltage drop due to gas diffusion resistance through the porous electrodes; (d) *cathode activation polarization*—the voltage drop associated with the electrochemical reduction of the active constituent in the oxidant (typically oxygen); (e) *anode activation polarization*—the voltage drop associated with the electrochemical oxidation of the active constituent in the

fuel (typically hydrogen). Finally, for practical experimental work on cells and stacks, a sixth loss mechanism exists due to reactant leakage. The degradation mechanisms introduced in Section 1 may affect one or more of these voltage drops. Further, some of these voltages play a greater role than others in determining the cell/stack performance. As a result, it is helpful in the analysis of degradation to separate these individual voltage losses from the overall voltage loss in order to focus attention on likely mechanisms for a given degradation study.

Challenges exist, however, in accurate separation of the polarization losses. This limitation hampers efforts to identify the dominant loss mechanism. In particular, with the exception of using elaborate reference electrodes, concentration polarizations are not directly and separately measurable, and must be calculated from other known or estimated parameters (i.e., free-stream reactant concentrations must be known). Additionally, activation polarizations can be difficult to separately measure for the thin electrolyte technology used in contemporary cells, Mogensen et al. [20]. In spite of these difficulties, it is helpful to consider these five overpotentials as the basic loss parameters for characterizing cell operation. Hence, the present work employs a model from the literature (see Section 4 and Appendix A) that separately characterizes these loss mechanisms.

Further improvements in cell performance will also be aided by improved diagnostic capability and test methods that enable separate measurement of the various polarization losses. Such capability will improve developers' knowledge of the relationship between material and microstructural effects and operating conditions.

3. Assessing degradation

As described in Section 2, we use measured voltage losses to assess degradation performance of the fuel cell. To help explain the precise methodology proposed here, a model for the cell voltage degradation will first be presented. Using the results of the model predictions, a demonstration of the proposed method of assessing degradation will be provided.

3.1. Cell voltage model

Several detailed models [21–23] have been developed which account for voltage losses due to gas transport through porous electrodes, electrochemical reactions at the electrodes (near electrode–electrolyte interfaces), and material ohmic resistance. Here, we extend the model of Virkar et al. [23] (see Appendix A) to include losses due to reactant leakage:

$$V(i,t) = (E_N - \eta_L) - (iR_i + \eta_{aa} + \eta_{ac} + \eta_{ca} + \eta_{cc}) \quad (1)$$

In Eq. (1), V is the cell voltage, i is the average cell current density, t is the time, E_N is the ideal Nernst potential, $E_N = E^\circ + RT/n \ln(\Pi \text{react}^\nu / \Pi \text{product}^\nu)$, η_L is the loss due to reactant leakage, η_{aa} and η_{ac} are the activation overpotentials for the anode and cathode, respectively, η_{ca} and η_{cc} are the concentration overpotentials for the anode and cathode, respectively, and R_i is the total resistivity of all cell components. E° is the standard state voltage, n is the number of electrons transferred, and product$^\nu$ and react$^\nu$ are the product and reactant activities raised to their stoichiometric coefficients, ν, respectively. At zero current, $V(0,t) = E_N - \eta_L$ which is the open circuit voltage (OCV) which we denote as E_o. Hence, the loss parameters grouped on the far right side of Eq. (1) contribute to the voltage deviation from E_o. All of these loss parameters are functions of current, operating temperature (T) and pressure (P), and reactant compositions. Because of this, we recommend (see following discussion) that the thermodynamic state of a cell under test be fixed (e.g., T, P, and fuel composition held constant.) Finally, each of the six loss parameters of Eq. (1) can change with time (degrade), and therefore the cell voltage, V, is also a function of time as shown in Eq. (1).

3.2. ASR as a performance parameter

It is common in the literature to find use of what is referred to as ASR. This parameter is sometimes defined locally at a specific current, i_s, by taking the derivative of Eq. [1] with respect to current density, i, as $\text{ASR}'(i,t) = \mathrm{d}V(i,t)/\mathrm{d}i$. A limitation of this definition is that it does not account for losses occurring at current less than i. As a result, the derivative method for ASR cannot account for the overall accrued losses of the cell (from $i = 0$ to $i = I$), and therefore will not provide a relevant assessment of cell performance at some current level I. For the purposes of assessing performance, and to allow for a comparison between different cell technologies operated at a relevant current density, i, an improved definition in terms of Eq. (1) is:

$$\text{ASR}(i,t) = \frac{E_0(t) - V(i,t)}{i} \quad \text{or,} \quad \text{ASR}(i,t) = \frac{R_i i + \eta_{aa} + \eta_{ac} + \eta_{ca} + \eta_{cc}}{i} \quad (2a)$$

This definition removes loss effects due to reactant leakage and variable reactant mixture supply (inherent in any experiment), and can be helpful if one is focused on the performance of cell materials (e.g., modifications in electrode structure). On the other hand, if the focus is total cell performance (cell material + seal technology), then the reference potential should be the Nernst voltage:

$$\text{ASR}(i,t) = \frac{E_N(t) - V(i,t)}{i} \quad \text{or,} \quad \text{ASR}(i,t) = \frac{\eta_L + R_i i + \eta_{aa} + \eta_{ac} + \eta_{ca} + \eta_{cc}}{i} \quad (2b)$$

This definition includes the loss effects of reactant leakage, but continues to remove loss effects due to variable reactant mixture supply.

The formulation given by Eqs. (2a) and (2b) provides the *overall* (*or integral*) *loss* in performance when operating at a given current, and is a 'linearization' from $i = 0$ to $i = I$ of the individual overpotentials. From a mathematical perspective, it provides an *average* measure of the local ASR from $i = 0$ to $i = I$. This is in contrast to the *local incremental loss* in performance if ASR is assessed using the differential of the voltage–current curve. These distinctions are highlighted in Fig. 5, and will be discussed fully in Section 4 where an example case is studied.

The specific application (single cell vs. stack) and objectives of the research (assessing electrode performance vs. total cell), will dictate which form of Eqs. (2a and 2b) is needed. To provide simplicity in the present discussion, we will focus on the use of E_N as the reference voltage for ASR.

Benefits and Limits of ASR(i,t) as a Performance Parameter—one benefit of using ASR(i) as defined in Eqs. (2a) and (2b) is that its value is less sensitive to operating conditions. Performance effects due to gas composition differences between two experiments or drift over the course of a single long experiment can be dampened by adoption of Eqs. (2a) and (2b)—this is one of the key advantages to the presently recommended definition of ASR for performance assessment. The dampening of gas composition variations results from the fact that the ASR(i,t) calculation subtracts the effect of E_N (which is a function of gas composition) on the operating cell voltage. By removing experimental variations, a reduction in experimental noise may be possible, which can help

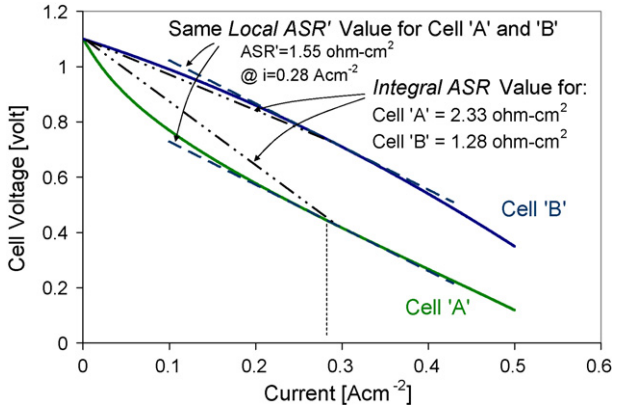

Fig. 5. Simulated *V–i* data from two different cells having same local ASR′ at 0.28 A cm^{-2}. While a local ASR′ analysis shows equivalent cell performance, Cell 'A' clearly has poorer performance—this fact is captured in the higher overall (integral) ASR evaluation.

to minimize the required test duration—see discussion surrounding Fig. 4.

A perceived limitation of ASR(i) as defined in Eqs. (2a) and (2b) is that it is a function of current, rather than being purely a material property. While a current independent definition of ASR would be desirable (Steinberger-Wilckens et al. [2]), at present it is unclear how such a parameter would be generally viable. One qualification in the use of Eqs. (2a) and (2b) is that it requires that the dominant loss mechanism(s) not be strongly affected by gas composition. If they are affected by gas composition, then the data obtained will be biased by those effects regardless of the 'corrections' to gas variability offered by Eqs. (2a) and (2b). The critical point identified here is that when technology comparisons are being performed to assess degradation, testing should be done at similar thermodynamic conditions and current density to minimize possible secondary effects, and best allow a correction of remaining anomalous variations using Eqs. (2a) and (2b). Doing so ensures the best available performance measure is achieved.

In summary, ASR as expressed in Eqs. (2a) and (2b) fully accounts for all cell losses in an integral sense. It also offers a way to minimize some of the sources of experimental noise. Furthermore, it is time dependent, and, therefore, it can also be used to evaluate degradation for the cell/stack as described in the next section.

3.3. Constant current, constant voltage and constant power measurements

Due to the lack of degradation measurement standards, there presently exists a variety of methods used to measure and report cell performance and degradation. Constant current and constant voltage are the most commonly used methods, but constant power could also be used which would result in an inversely proportional change in both current and voltage as the cell degrades.

To avoid complicated experimental procedures, and thereby improve experimental data quality, the use of constant thermodynamic conditions (T, P, and reactant composition) is recommended. This produces a tractable program of experimental development whereby effects of operating condition on degradation can also be studied. Further, when constant current is specified, the overall reactant utilizations will be fixed. Since overall reactant utilizations govern the overall boundary conditions for material oxidation potential, constant oxygen partial pressures on both anode and cathode can be achieved. If such constant oxidation potentials were not achieved (as occurs in constant voltage and power measurements), then changes in ceramic oxide material states could be induced, resulting in a secondary source of induced degradation. In short, constant flow conditions, and constant current conditions will best allow constant thermodynamic conditions to exist throughout the test and therefore will prevent variable operating conditions from biasing degradation rates.

While constant current and flow conditions achieve a constant overall oxidation potential boundary condition as explained above, voltage is itself a thermodynamic parameter. It must remain clear that as degradation results in various increased overpotentials (resulting in local voltage changes), it may be possible for such local voltage changes to affect the loss behavior. Even so, such potential coupling between a fundamental degradation mechanism and local overpotential changes are all kept 'local'. The alternative constant voltage testing could broaden the coupling to other areas of the cell.

3.4. Degradation rate: ASR vs. time

We begin the analysis of degradation by considering the limit where the degradation approaches zero. Without degradation, the cell voltage and ASR are constant for a particular system current density, i_s. According to Eqs. (2a) and (2b), on a steady-state *V–i* curve, the voltage, $V(i)$, at any current, i_s, can be given by:

$$V(i_s) = E_N - \mathrm{ASR}(i_s) i_s \tag{3}$$

Now, for finite degradation, we hypothesize that at some time, t_o, and at some constant operating system current density, i_s, the fuel cell begins to degrade. ASR begins to change with time (and hence operating voltage as well). During this time period of decay, the voltage change with time referencing the initial starting voltage can be given by:

$$V(i_s, t) - V(i_s, t_o) = -i_s(\mathrm{ASR}(i_s, t) - \mathrm{ASR}(i_s, t_o)) \tag{4}$$

where

$$V(i_s, t_o) = E_N - \mathrm{ASR}(i_s, t_o)_i i_s \tag{5}$$

and where we assume that nominal reactant supply composition is constant, thereby making $E_N(t_o) = E_N(t)$. Dividing Eq. (4) by time $(t - t_o)$ one obtains a decay rate in units of volts per unit time. In the limit of infinitesimal time change, one obtains the *instantaneous degradation rate* given by:

$$\frac{\mathrm{d}(V(i_s, t))}{\mathrm{d}t} = -\frac{\mathrm{d}(\mathrm{ASR}(i_s, t))}{\mathrm{d}t} i_s \tag{6}$$

Eq. (6) is the absolute voltage degradation rate at current i_s, and time t. In terms of % per hour:

$$\mathrm{DR}(t) = -100 \times \left(\frac{\mathrm{d}V(i_s, t)/\mathrm{d}t}{V(i_s, t_o)} \right) = 100 \times \left(\frac{\mathrm{dASR}(i_s, t) i_s/\mathrm{d}t}{V(i_s, t_o)} \right) \tag{7}$$

Returning again to a finite time change $(t - t_o)$, an overall *average degradation rate* can be obtained, $m = (V(i_s,t_o) - V(i_s,t))/(t - t_o)$. The degradation rate is often calculated by such linearization of the entire voltage vs. time curve to provide one number for the average degradation rate over the duration of the test. Such linearization of the voltage vs. time curve has been suggested previously Vinke [24], and may be necessary for noisy experimental data. Again, in terms of % per hour, the average degradation rate is given by:

$$\overline{\mathrm{DR}}(t) = 100 \frac{V(i_s, t_o) - V(i_s, t)}{V(i_s, t_o) \times (t - t_o)} = 100 I_s \frac{\mathrm{ASR}(i_s, t) - \mathrm{ASR}(i_s, t_o)}{V(i_s, t_o) \times (t - t_o)} \tag{8}$$

The two forms of degradation rate (average and instantaneous) will be compared later in Section 4 where an example is given for the method of degradation analysis being proposed (see Fig. 8).

3.5. Normalized vs. absolute degradation rate

The present paper focuses on the use of the normalized degradation rate parameter as shown in Eqs. (7) and (8). Two views of such normalization can be taken.

- *Pro*: A normalized degradation as given here directly relates to fuel efficiency changes, and as such it establishes a rate schedule for increases in fuel consumption (and costs) following startup—a very relevant concern to end users. To be clear, it is the lifetime cost that is the primary concern of the end user, and both the initial performance (e.g., efficiency) and the relative degradation rate of a given unit must be described. Eqs. (7) and (8) provide a meaningful degradation parameter for this purpose, and, therefore, the authors feel that a valid need for a normalized degradation rate parameter is clear.
- *Con*: The normalization of the degradation rate as shown in Eqs. (7) and (8) has been considered by Steinberger-Wilckens et al. [2]. As they point out, such normalization can result in higher apparent degradation rate values for cells operated at lower voltages (vs. a baseline) where in fact the same absolute voltage per unit time decay rate may occur as for the baseline. (Normalizing by a lower numerical value will bias the degradation rate high.) The normalized degradation rate gives a combined/mixed assessment of low voltage performance and absolute degradation rate, rather than a pure assessment parameter for degradation rate alone. Further, as noted by Vinke [24], the normalized degradation rate as defined here is not a material-based parameter, but includes information on operating conditions as well.

Thus far, however, no general material specific degradation parameter has been proposed. Even the ASR, as defined by Eqs. (2a) and (2b), is not (in general) a material specific property—a fact that is clear given that concentration losses depend on thermodynamic operating conditions. Finally, it remains questionable that an absolute degradation rate would resolve all the issues identified on the normalization approach, and may have issues of its own. For example, if it happens that two cells have the same degradation rate, but one is operated at a significantly lower voltage than the other, fair performance comparisons are complicated. Operation of cells at similar thermodynamic conditions is desired to avoid secondary effects, and such is not generally possible if the voltages are significantly different.

Clearly more work, both theoretical and experimental, is needed to help navigate these remaining challenges. For the remainder of the paper, we will focus on the use of the normalized degradation parameter calculation given by Eqs. (7) and (8) as it appears to have use regardless of future developments.

4. Cell degradation model and application to degradation assessment

To provide a clear application of the degradation assessment method proposed above, a prediction for ASR vs. time was developed following a common phenomenological model for fuel cell performance proposed by Virkar et al. [23], the details of which are provided in Appendix A. (For this model, losses due to leakage are ignored.) The model provides data for predicting the behavior of a cell under long-term decay, and those results will be used to demonstrate the proposed degradation assessment method.

4.1. The model

The model uses the parameters shown in Eq. (1) (sans leakage loss) for predicting a steady-state $V(i)$ relationship, the results of which are shown in Fig. 6. From these data, the steady-state ASR(i) as given by Eq. (2a) will be:

$$\mathrm{ASR}_{ss}(i_s) = \frac{R_i i_s + \eta_{aa} + \eta_{ac} + \eta_{ca} + \eta_{cc}}{i_s}$$

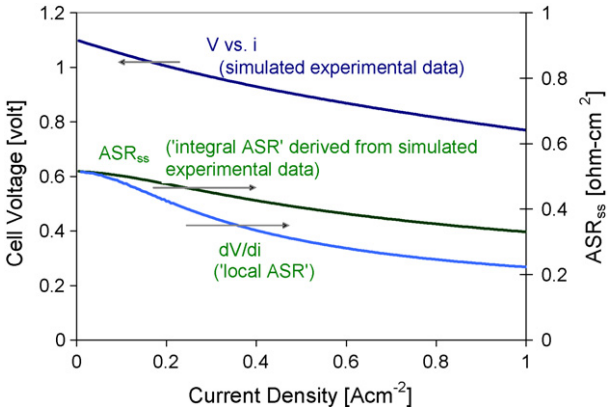

Fig. 6. Simulated steady-state $V(i)$ curve (prior to decay) following model of Virkar et al. [23]. Steady-state $\mathrm{ASR}_{ss}(i)$ calculated from given $V(i)$ data. Also shown is the local ASR calculated from the derivative of $V(i)$. As the figure shows, the integral ASR method provides an improved measure of performance as it takes into account the entire decay.

This steady-state ASR result is also shown in Fig. 6. To highlight the difference between this 'integral' ASR and one defined using a 'local analysis' via the derivative, Fig. 6 also shows ASR calculated from the derivative of $V(i)$. It is found that the two definitions provide the same result at low current (since E_N is also the OCV condition), but begin to deviate significantly at higher currents, ca. $i > 0.15\ \mathrm{A\,cm^{-2}}$. For $i > 0.25\ \mathrm{A\,cm^{-2}}$, however, the difference between the two values is largely constant, which can be understood given the relatively straight $V(i)$ line over the range of i given. Should strong diffusion limits (inducing curvature in $V(i)$) be exhibited in the $V(i)$ curve, then the deviations between ASR values would become very large. In addition, if E_N was greater than OCV (often the case where reactant leakage may occur), then the 'integral' ASR based on Eq. (2b) would likely be greater than the 'local' ASR at low currents thereby causing further deviation between curves.

To evaluate degradation, we now assume a case where long term steady loading of the cell occurs (as in typical degradation studies) and where the cell current is fixed at $i_s = 0.7\ \mathrm{A\,cm^{-2}}$. The initial ASR_{ss} for this condition is $0.37\ \Omega\,\mathrm{cm}^2$ as shown in Fig. 6. For some degradation mechanism, we assume that decay begins at some time t_o so as to increase the ASR with time. A decay mechanism having an exponential increase vs. time is assumed; hence, the time varying ASR(i_s,t) was modeled by multiplying the steady-state ASR_{ss} by $e^{(kt)}$, where k is the ASR growth constant. Specifically:

$$\mathrm{ASR}(i_s, t) = (e^{(k(t-t_o))})\mathrm{ASR}_{ss}(i_s) \quad (9)$$

The factor $(t - t_o)$ in the exponent accounts for the fact that degradation in the cell/stack begins after some initial time t_o as explained in Section 3b. Assuming an exponential growth constant, k, of $3\%\ \mathrm{kh^{-1}}$, $t_o = 0.0$ h and a current density of $i = 0.7\ \mathrm{A\,cm^{-2}}$, ASR($0.7\ \mathrm{A\,cm^{-2}}$, t) was calculated as shown in Fig. 7. Using Eq. (3) the cell voltage vs. time at $0.7\ \mathrm{A\,cm^{-2}}$ can be calculated, which is also shown in Fig. 7.

4.2. Assessing degradation

The above degradation model provided $V(t)$ data for a cell under long term testing. From this data, the voltage degradation rate was generated using Eqs. (7) and (8), for the instantaneous DR(t) and average $\overline{\mathrm{DR}}(t)$, respectively. Both of these values are presented in

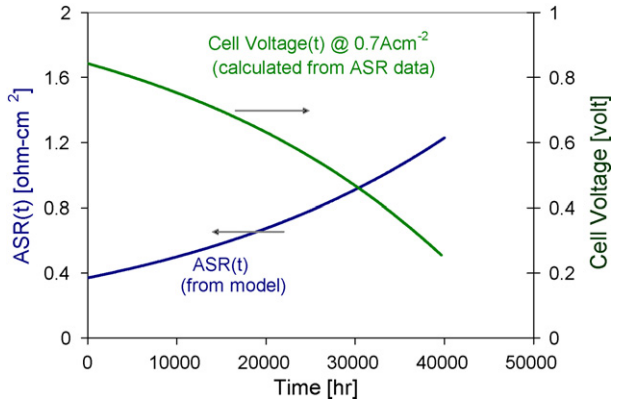

Fig. 7. Modeled ASR(t) at $i_s = 0.7\ \mathrm{A\,cm^{-2}}$. Assumed degradation phenomena having exponential growth constant, k, of 3% $\mathrm{kh^{-1}}$, $t_o = 0.0$ h. Resultant $V(t)$ given by Eq. (5).

Fig. 8. As seen in the Figure, over the time evaluated, $\overline{\mathrm{DR}}(t)$ ranges between 0.9% per 1000 h and 1.8% per 1000 h, and is lower than the instantaneous DR(t) for the case studied.

5. Degradation assessment from experimental data

Available experimental data is employed for the examination of cell ASR performance and degradation rate—Steinberger-Wilckens et al. [2]. Long-term data (ca. 7500 h) on a short stack was taken by Juelich to assess integrated component (full cell) degradation. Long term data was also taken on individual cells to focus on the effect of interconnect coating performance.

Fig. 9 shows the ASR and average degradation rate calculated from the Juelich data using Eqs. (2a) and (2b) on a short stack operated at a constant current of 0.3 $\mathrm{A\,cm^{-2}}$ at 800 °C. The data are from a two-cell SOFC stack with cell size 20 cm × 20 cm. As can be seen from the figure, the cell voltage gradually decays over time, and the calculated ASR increases accordingly. The stack average degradation rate is high at the start of the test (ca. 20% $\mathrm{kh^{-1}}$), but gradually lowers to an acceptable rate (ca. 1% $\mathrm{kh^{-1}}$) after 5000 h. This behavior is similar to that shown in Fig. 2 for the effect of H_2Se trace contaminant on cell operation, and is to be expected for degradation mechanisms that initially force changes in the voltage performance, but then stabilize thereby leaving the cell in a fixed (decayed) state.

Fig. 10 shows the ASR data obtained from the Juelich data on interconnect performance where one cell was tested with a coated interconnect and one was tested without a coating. The cell ASR without a coating is severe (as high as 2 Ω $\mathrm{cm^2}$), while with a protective coating ASR values remain below 0.6 Ω $\mathrm{cm^2}$. While it is readily

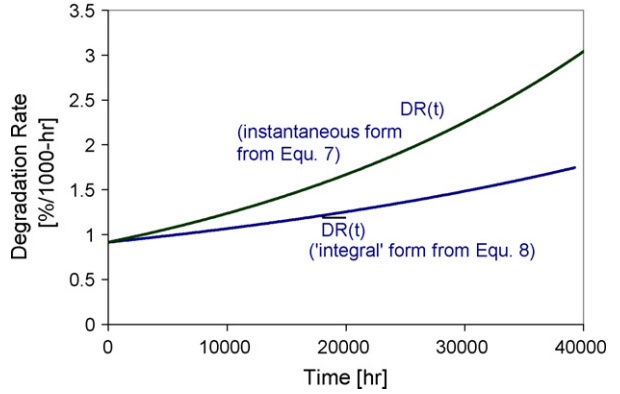

Fig. 8. Resultant degradation rates for modeled example study as calculated from ASR(t) data of Fig. 4 using Eqs. (7) and (8).

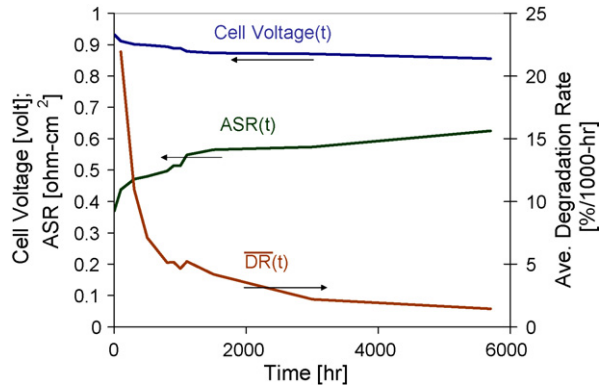

Fig. 9. Juelich experimental cell voltage data from a short stack test—Ref. Steinberger-Wilckens et al. [2]. $H_2 = 90\%$, $H_2O = 10\%$, low utilization, $E_N \sim 1.043$ V. Calculated ASR(t) and average degradation rate also shown.

apparent from such data which cell operated the best (given the extremely different performance), as cell technology improves and ASR values diminish and become similar in magnitude, the importance of correcting for test conditions (E_N) will be more valuable for reducing test time requirements—see discussion surrounding Fig. 4.

6. Discussion

Our goal is to improve degradation assessment methods, and to propose a definition for ASR that allows the greatest utility. Specifically, for evaluating ASR at a given current we propose to reference cell performance to either the open circuit voltage (E_o), or the ideal cell potential (E_N). By referencing the cell to the open circuit voltage, corrections for test conditions can be achieved, and variations in seal behavior can be removed from the case-to-case ASR comparisons. As an example, OCV would be suited as a reference for work focused on electrode-to-electrode performance comparisons, and would remove voltage loss effects attributed to seal leaks. On the other hand, by using the ideal potential as a reference, the effects of seal degradation (e.g., leakage) over time can also be captured in the ASR data, which is important for stack level studies.

The application of ASR was demonstrated in Section 5 from available experimental data. In the application of the analysis for ASR, the performances of two different cells were compared in regard to the effect of interconnect coating. Assuming similar

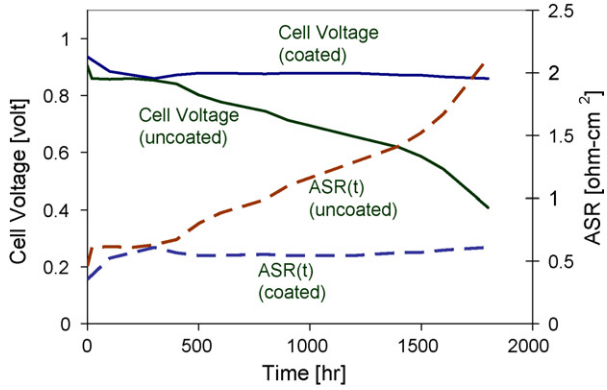

Fig. 10. Juelich experimental cell voltage data for interconnect coating comparison study—Ref. Steinberger-Wilckens et al. [2]. Calculated ASR values ($E_N = 1.043$ V assumed) for the coated and uncoated interconnects are also shown. The coated and uncoated sample ASR values are best compared via a correction for test variations as described in the text.

conditions for testing, the ASR values were calculated. The ASR performance of the coated interconnect was clearly better. While the given example did not require close scrutiny to assess relative performance (the cells showed extremely different behavior), in general comparisons may not be so obvious, and accurate analysis is required to determine which technology is best. Further, an ASR method that removes unwanted experimental effects (e.g., seal losses) improves the accuracy of comparisons. The ASR described here enables such corrections.

For assessing degradation rates, we choose to normalize the degradation rate, DR, by the initial cell voltage so as to provide a performance parameter that will be meaningful to end-user interests. As noted by others, this will bias (toward high values) cells operated at low voltage but having the same absolute degradation as cells operated at high voltage. However, it appears that no alternative methodology for making practical and meaningful determinations for degradation exists. The use of an *absolute degradation rate* does not provide benefits that generally apply to a wide variety of cases.

The application of DR was demonstrated in Section 5 from available experimental data. In the application of the analysis for DR, the average degradation rate, $\overline{\mathrm{DR}}(t)$, for a short stack was determined. $\overline{\mathrm{DR}}(t)$ was found to decrease over time, and at the end of the test period had a value of about 1.4% per 1000 h. From the stack data, it would appear that if the test continued, values below 1% per 1000 h could be achieved. This value of $\overline{\mathrm{DR}}(t)$ for the Juelich technology can be compared to other cell technology to determine best overall performance during the lifetime of a given SOFC generator.

Given their respective benefits and limitations, ASR and DR should be applied appropriately. In short, for making fair comparisons in the performance of a given cell component, e.g., as in interconnect coating comparisons, ASR should be used. For making comparisons at the full cell (or stack) level, DR can be used. For the former, proper corrections for possible anomalous test conditions can be made. For the latter, where the attention to fuel efficiency performance is the key issue, DR can be meaningfully used.

Finally, while the flexibility in the form of ASR (Eq. (2a) vs. Eq. (2b)) can be helpful in meeting the specific needs of the researcher on a case-by-case basis, it will require that results be carefully presented and interpreted so as to avoid improper interpretation of the results.

7. Summary and conclusion

Degradation remains an important issue for fuel cell technology. This paper reviews of some of the known cell/stack degradation issues, and proposes a method of evaluating both the degraded performance, and the rate at which degradation occurs. The two parameters identified are the ASR, and the DR, respectively. The ASR is defined as:

$$\mathrm{ASR}(i,t) = \frac{E(t) - V(i,t)}{i}$$

where E can be either OCV potential or the ideal Nernst potential depending on the needs of the researcher to remove certain experimental effects. The average degradation rate can be given by:

$$\overline{\mathrm{DR}}(t) = 100\frac{(V(i_\mathrm{s},t_\mathrm{o}) - V(i_\mathrm{s},t))}{V(i_\mathrm{s},t_\mathrm{o}) \times (t - t_\mathrm{o})}$$

The two definitions are exercised using both modeled and available experimental data. Specific conclusions are:

- For proper comparisons, testing should be done at similar thermodynamic conditions (constant T, P and reactant composition) and current density to minimize possible secondary effects and best allow a correction of remaining anomalous variations using Eqs. (2a) and (2b). The proposed definitions for ASR allow for the correction of thermodynamic variations in test conditions and allow for improved accuracy when comparing test results.
- The flexibility in the form of ASR (Eq. (2a) vs. Eq. (2b)) can be helpful in meeting specific test needs, but results must be carefully presented so as to avoid improper interpretation.
- ASR is best used for developers as they compare the performance of one technology to another (e.g., the performance of different interconnect coatings).
- DR is normalized by the initial operating voltage, and is best suited for full cell and stack performance comparisons where degradation and cell performance are both critical. In particular, it will allow end-users to better compare different commercial generator systems in regards to their likely increased fuel costs over time.

The authors believe that the *benefits* of the method (facilitating accurate comparisons between cell data) will be demonstrated by its widespread application, resulting in proper identification of improved cell materials and designs. Even so, this topic would benefit from further discussion and development. Also, the assessment method proposed here requires further demonstration, and our work to improve degradation performance would benefit by determining its sensitivity to specific modes of degradation.

Acknowledgement

The authors would like to acknowledge the help of Mr. Edward Robey on the statistical analysis reported in this paper.

Appendix A

The parametric phenomenological fuel cell performance model is fully developed in the Virkar [25], Virkar et al. [23] and Zhao et al. [26] papers for an anode-supported, atmospheric, 800 °C SOFC. The equations used were:

$$V(i,t) = E_0 - iR_\mathrm{i} - \eta_\mathrm{aa} - \eta_\mathrm{ac} - \eta_\mathrm{ca} - \eta_\mathrm{cc}$$

where, for the model given by Zhao,

$$\eta_\mathrm{ac} = \left(\frac{RT}{2F}\right)\mathrm{arcsinh}\left(\frac{i}{2i_\mathrm{OC}}\right)$$

$$\eta_\mathrm{aa} = \left(\frac{RT}{2F}\right)\mathrm{arcsinh}\left(\frac{i}{2i_\mathrm{OA}}\right)$$

$$\eta_\mathrm{cc} = -\left(\frac{RT}{4F}\right)\ln\left(\frac{P'_{\mathrm{O}_2(i)}(i)}{P^\mathrm{o}\mathrm{O}_2}\right)$$

$$\eta_\mathrm{ca} = -\left(\frac{RT}{2F}\right)\ln\left(\frac{P'_{\mathrm{H}_2(i)}(i)P^\mathrm{o}\mathrm{H}_2\mathrm{O}}{P'_{\mathrm{H}_2\mathrm{O}(i)}(i)P^\mathrm{o}\mathrm{H}_2}\right)$$

Variables used in the above equation are defined as:

- $R = 8.3144\ \mathrm{J\,K^{-1}\,mol^{-1}}$ (universal gas constant)
- $R_\mathrm{i} = \delta/\sigma$ (cell ohmic resistance (electrolyte and all other layers))
- $\delta = 0.01$ cm (the thickness of the electrolyte in this example—the ohmic resistivity of the anode and cathode, interconnect layers and other inter-layers are neglected)
- $\sigma = 0.1\ \mathrm{S\,cm^{-1}}$ (electrolyte conductivity)
- $i_\mathrm{OA} = 0.2\ \mathrm{A\,cm^{-2}}$ (limiting current anode)
- $\mathrm{i}_\mathrm{OC} = RT/\{4F(d\rho_\mathrm{i}\rho_\mathrm{ct}/((1-V_\mathrm{v})L_\mathrm{tpb}))^{1/2}\}$ (limiting current cathode)
- $F = 96{,}485\ \mathrm{C\,mol^{-1}}$ (Faraday constant)
- $T = 1073$ K (cell temperature)
- $d = 1\ \mu\mathrm{m}$ (grain size of composite electrode)
- $\rho_i = 30\ \Omega\,\mathrm{cm}$ (ionic resistivity of the composite electrode)

- $\rho_{ct} = 126{,}000\ \Omega\,cm$ (charge transfer resistivity)
- $V_v = 0.25$ (volume fraction porosity)
- $L_{tpb} = 10{,}000\ cm^{-1}$ (length triple phase boundary)
- $P'_{O_2(i)}(i)$ = partial pressure of O_2 close to the electrolyte – cathode interface $= P_{O_2(i)}(i) - M$
- $P'_{O_2(i)}(i) = P^o_{O_2} - (iRT/4F)((P_c - P^o_{O_2})/P_c)(L_{c(1)}/D^{eff(1)}_{O_2-N_2})$
- $M = ((P^o_{O_2} - P_{O_2(i)}(i))/(P_c - P^o_{O_2})) \times (P_c - P_{O_2(i)}(i))((D^{eff(1)}_{O_2-N_2} L_{c(2)}/L_{c(1)})/D^{eff(2)}_{O_2-N_2})$
- $P^o_{O_2} = 0.21$ ATM (partial pressure of oxygen just outside the cathode)
- i = current density
- $P_c = 1$ ATM (total cathode gas pressure)
- $L_{c(1)} = 20\ \mu m$ (thickness cathode current collector)
- $D^{eff(1)}_{O_2-N_2} = 0.14\ cm^2\ s^{-1}$ (effective binary diffusivities through the cathode collector)
- $L_{c(2)} = 2\ \mu m$ (thickness cathode functional layer)
- $D^{eff(2)}_{O_2-N_2} = 0.14\ cm^2\ s^{-1}$(effective binary diffusivities through the cathode interlayer)
- $P^o_{H_2} = 0.97$ ATM (partial pressure of H_2 just outside anode support)
- $P^o_{H_2O} = 0.03$ ATM (partial pressure of H_2O just outside anode support)
- $P_a = 1$ ATM (total fuel pressure)
- $P'_{H_2(i)}(i)$ = partial pressure of H_2 close to the electrolyte – anode interface $= P^o_{H_2} - (iRT/2F)(L_{a(1)}/D^{eff(1)}_{H_2-H_2O} + L_{a(2)}/D^{eff(2)}_{H_2-H_2O})$
- $P'_{H_2O(i)}(i)$ = partial pressure of H_2O close to the electrolyte – anode interface $= P^o_{H_2O} - (iRT/2F)(L_{a(1)}/D^{eff(1)}_{H_2-H_2O} + L_{a(2)}/D^{eff(2)}_{H_2-H_2O})$
- $L_{a(1)} = 50\ \mu m$ (thickness cathode current collector)
- $D^{eff(1)}_{H_2-H_2O} = 0.68\ cm^2\ s^{-1}$(effective binary diffusivities through the anode support)
- $L_{a(2)} = 2\ \mu m$ (thickness anode functional layer)
- $D^{eff(2)}_{H_2-H_2O} = 0.08\ cm^2\ s^{-1}$(effective binary diffusivities through the anode interlayer).

References

[1] R.S. Gemmen, Presented at the 2007 SECA Workshop, San Antonio, TX, August 7–9, 2007.
[2] R. Steinberger-Wilckens, L. Blum, H. Buchkremer, S. Gross, L. de Haart, K. Hilpert, H. Nabielek, W. Quadakkers, U. Reisgen, R. Steinbrech, F. Tietz, Int. J. Appl. Ceram. Technol. 3 (6) (2006) 470–476.
[3] S.K. Mazumder, K. Acharya, C.L. Haynes, R. Williams, M.R. von Spakovsky, D.J. Nelson, D.F. Rancruel, J. Hartvigsen, R.S. Gemmen, IEEE Trans. Power Electron. 19 (5) (2004).
[4] A. Ioselevich, A.A. Kornyshev, W. Lehnert, Solid State Ionics 124 (1999) 221–237.
[5] A.A. Kulikovsky, H. Scharmann, K. Wippermann, Electrochem. Commun. 6 (2004) 75–82.
[6] M.W. Fowler, R.F. Mann, J.C. Amphlett, B.A. Peppley, P.R. Roberge, J. Power Sources 106 (2002) 274–283.
[7] C. Haeringa, A. Roosena, H. Schichl, Solid State Ionics 176 (2005) 253–259.
[8] G. Meyer, G. Gebel, L. Gonona, P. Capron, D. Marscaq, C. Marestin, R. Mercier, J. Power Sources 157 (2005) 293–301.
[9] M. Schulze, C. Christenn, Appl. Surf. Sci. 252 (2005) 148–153.
[10] A.W. Chen, G. Sun, J. Guo, X. Zhao, S. Yan, J. Tian, S. Tang, Z. Zhou, Q. Xin, Electrochim. Acta 15 (12) (2006) 2391–2399.
[11] M. Schulze, E. Gülzow, J. Power Sources 127 (2004) 252–263.
[12] S. Taniguchi, M. Kadowaki, H. Kawamura, T. Yasuo, Y. Akiyama, Y. Miyake, T. Saitoh, J. Power Sources 55 (1995) 73–79.
[13] A.C. Chervin, R.S. Glass, S.M. Kauzlarich, Solid State Ionics 176 (2005) 17–23.
[14] A. Taniguchi, T. Akita, K. Yasuda, Y. Miyazaki, J. Power Sources 130 (2004) 42–49.
[15] Y. Matsuzaki, I. Yasuda, Solid State Ionics 132 (2000) 261–269.
[16] L. Aguilar, S. Zhab, Z. Chengb, J. Winnick, M. Liu, J. Power Sources 135 (2004) 17–24.
[17] K.S. Weil, C.A. Coyle, J.T. Darsell, G.G. Xia, J.S. Hardy, J. Power Sources 152 (2005) 97–104.
[18] R.S. Gemmen, C.D. Johnson, J. Power Sources 159 (2006) 646–655.
[19] R. Steinberger-Wilckens, F. Tietz, M. Smith, J. Mougin, B. Rietveld, O. Bucheli, J. van Herle, R. Rosenberg, M. Zahid, P. Holtappels, in: K. Eguchi, S.C. Singhal, H. Yokokawa, J. Mizusaki (Eds.), Proceedings of the Solid Oxide Fuel Cells 10 (SOFC-X)—Part 1, Electrochem. Soc. Trans. 7 (1) (2007).
[20] M. Mogensen, P.V. Hendriksen, K.K. Hansen, in: J. Huijsmans (Ed.), Proceedings of the Fifth European Solid Oxide Fuel Cell Forum, vol. 2, Lucerne, Switzerland, July 1–5, 2002.
[21] A.C. Burt, L.B. Celik, R.S. Gemmen, A.V. Smirnov, J. Power Sources 126 (2004) 76–87.
[22] P. Aguiar, D. Chadwick, L. Kershenbaum, Chem. Eng. Sci. 57 (2002) 1665–1677.
[23] A.V. Virkar, M.C. Williams, S.C. Singhal, F. Zhao, Proceedings of the 30th Anniversary Volume of Fuel Cell Seminar, ECS Transactions, vol. 3, No. 1, 2007, pp. 401–422.
[24] I. Vinke, Proceedings Workshop on Degradation, Crete, Greece, September 20, 2007.
[25] A.V. Virkar, J. Power Sources 172 (2007) 713–724.
[26] F. Zhao, A.V. Virkar, J. Power Sources 141 (2005) 79–95.
[27] A. Hagen, R. Barfod, P. Vang Hendriksen, Y. Liu, S. Ramousse, J. Electrochem. Soc. 153 (6) (2006) A1165–A1171.
[28] E. De Castro, Fuel Cells Durability & Performance, 2nd Edition Proceedings, The Knowledge Press, Inc., 2007.